Support Information

3d Transition Metal Coordination on Monolayer MoS_2: A facile doping method to functionalize surfaces

He Liu[1,†], Walner Costa Silva[2,†], Leonardo Santana Gonçalves de Souza[2], Amanda Garcez Veiga[2], Leandro Seixas[3,4], Kazunori Fujisawa[5,6,7], Ethan Kahn[8], Tianyi Zhang[8], Fu Zhang[8], Zhuohang Yu[8], Katherine Thompson[1], Yu Lei[8], Christiano J. S. de Matos[3,4], Maria Luiza M. Rocco[2], Mauricio Terrones[1,6,7,8,*], Daniel Grasseschi[2,*]

Affiliations

[1]Department of Chemistry, The Pennsylvania State University, University Park, PA, 16802.

[2]Institute of Chemistry, Federal University of Rio de Janeiro (UFRJ), 21941-909, Rio de Janeiro, Brazil.

[3]MackGraphe-Graphene and Nanomaterials Research Center, Mackenzie Presbyterian Institute, 01302-907, São Paulo, Brazil.

[4]Engineering School, Mackenzie Presbyterian University, 01302-907, São Paulo, Brazil.

[5]Research Initiative for Supra-Materials (RISM), Shinshu University, 4-17-1 Wakasato, Nagano, 380-8553, Japan.

[6]Department of Physics, The Pennsylvania State University, University Park, PA, 16802.

[7]Center for 2-Dimensional and Layered Materials, The Pennsylvania State University, University Park, PA, 16802.

[8]Department of Materials Science and Engineering, The Pennsylvania State University, University Park, PA, 16802.

† - Equal contributors

* - Corresponding authors

Table S1: Calculated adsorption energy (E_{ads}), M-Mo distance and M-S bond length for first row transition metal coordination on surface

Element	e Config	E_{ads} (eV)	M-Mo (Å)	M-S (Å)
Sc	$3d^1 4s^2$	-2.74	3.32	2.31
Ti	$3d^2 4s^2$	-3.02	2.99	2.32
V	$3s^3 4s^2$	-2.88	2.84	2.28
Cr	$3d^5 4s^1$	-1.58	3.06	2.38
Mn	$3d^5 4s^2$	-1.41	2.96	2.35
Fe	$3d^6 4s^2$	-2.64	2.52	2.13
Co	$3d^7 4s^2$	-3.05	2.85	2.06
Ni	$3d^8 4s^2$	-3.85	2.58	2.13
Cu	$3d^{10} 4s^1$	-1.73	2.83	2.25
Zn	$3d^{10} 4s^2$	-0.40	4.13	3.16

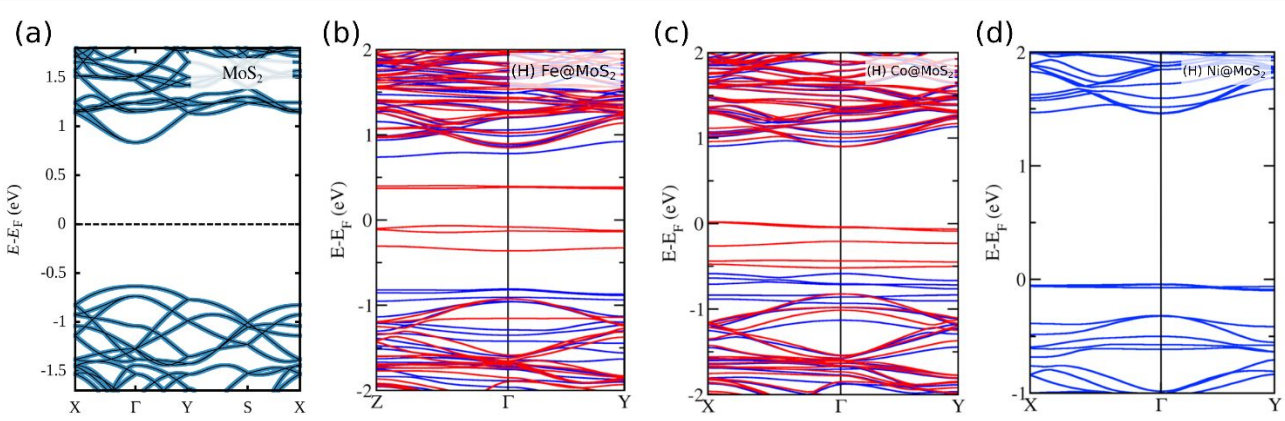

Figure S1: *Electronic Band Dispersion of MoS2 (a) and Fe (b), Co (c) and Ni (d) functionalization on H site. The blue and red curves indicate states with different spin polarization.*

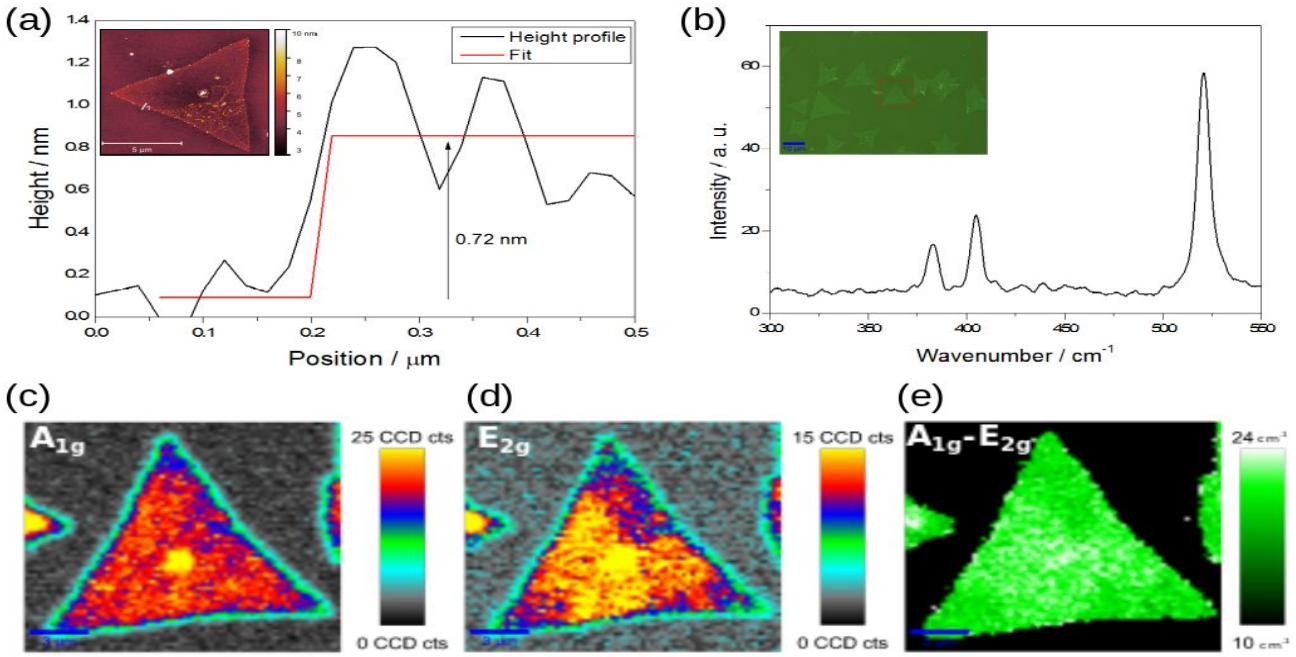

Figure S2: AFM image and height profile for MoS_2-Ni samples (a). Optical microscopy of MoS_2-Ni samples on inset (a,b). Raman spectra (b) and Raman mapping showing the A_{1g} (c) and E_{2g} (d) peaks intensity, and A_{1g} and E_{2g} wavenumber difference of MoS_2-Ni samples (e).

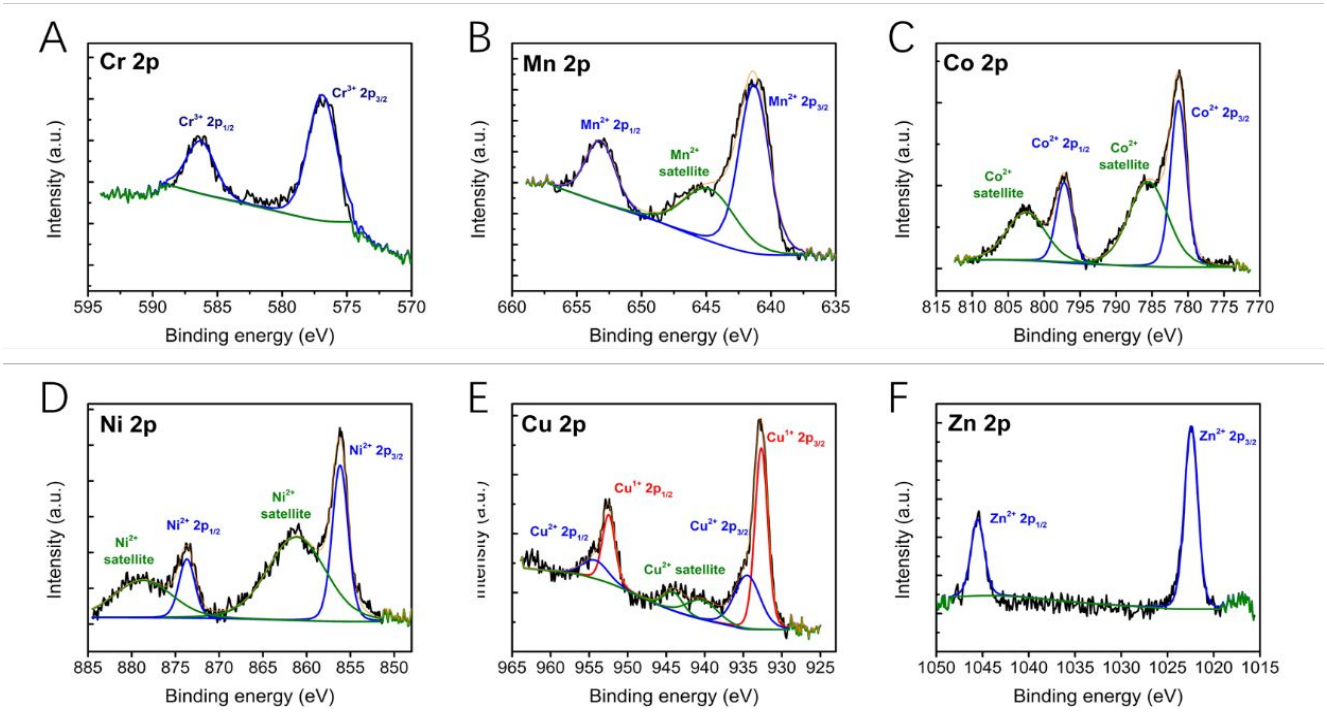

Figure S3: *XPS spectra of TM 3d orbit after functionalization. (A) Cr 2p orbit of Cr-MoS_2. The black curve is the original spectra after C1scalibaration. The blue curves are fitted to Cr^{3+} $2p_{1/2}$ and $2p_{3/2}$ peaks and they match perfectly with the original spectra. (B) Mn 2p orbit of Mn-MoS_2. The blue curves show the fitted Mn^{2+} peaks. In addition to the fitted Mn $2p_{1/2}$ and $2p_{3/2}$ peaks, a Mn satellite peak is also visible in the green curve. (C) and (D)Co and Ni 2p orbit of Co-MoS_2 and Ni-MoS_2. Similar satellite peaks could be fitted in addition to the Co^{2+} and Ni^{2+} peaks. (E) Cu 2p orbit of Cu-MOS_2. Here the spectra are fitted into 3 groups. The Cu^{1+} 2p peaks in red, the Cu^{2+} 2p peaks in blue and the Cu^{2+} satellite peaks in green. The presence of the Cu^{1+} peaks indicate a reduction reaction between the Cu^{2+}precusor and MoS_2. Similar to that of Au and MoS_2. (F)Zn 2p orbit of Zn-MoS_2 showing a perfect fit of Zn^{2+} $2p_{1/2}$, $2p_{3/2}$ and the original spectrum.*

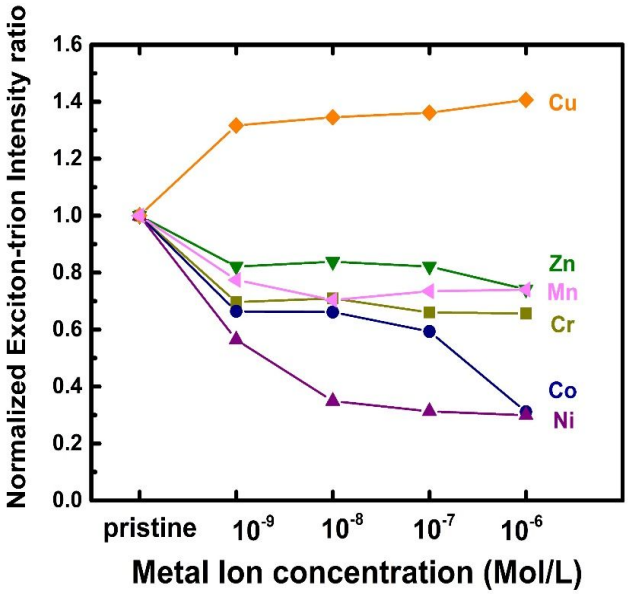

Figure S4: *Normalized exciton to trion intensity changes showing the percent change in exciton to trion ratio for various TM functionalized MoS_2 samples at different TM concentrations. The TMs here can be separated into 3 groups. One is Cu, which is showing an increase to the exciton to trion ratio, indicating p-type doping on the MoS_2. The second group is Zn, Mn and Cr where we see a small decrease in the ratio, indicating weak n-type doping of MoS_2. The last group is Co and Ni where we see a large decrease in the ratio that corresponds to strong n-type doping of MoS_2.*

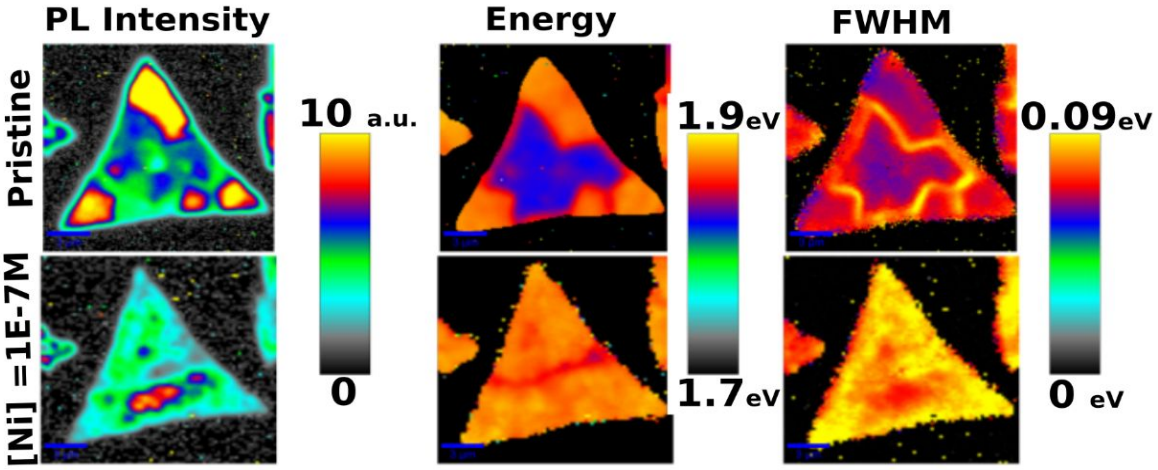

Figure S5: *Photoluminescence mapping showing the PL intensity, energy of the maximum intensity, and the peak full width at half maximum (FWHM) of Pristine and Ni functionalized MoS_2. Intensity changes are uniform through the whole flake, thus indicating homogenous dispersion onto the flake's surface.*

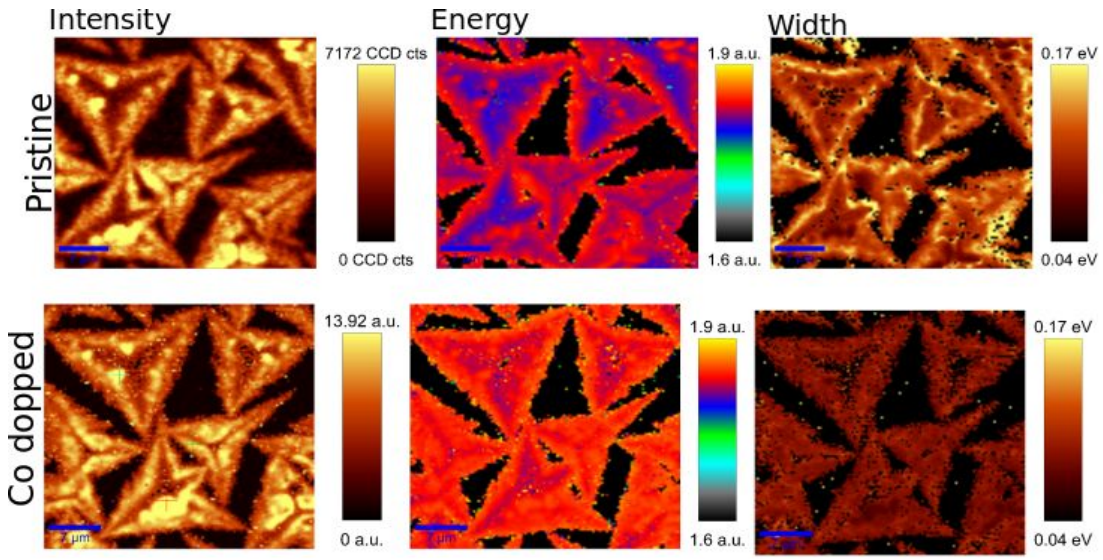

Figure S6: *Photoluminescence mapping showing the PL intensity, energy of the maximum intensity, and the peak full width at half maximum (FWHM) of Pristine and Co functionalized MoS2. Intensity changes are uniform through the whole flake, thus indicating homogenous dispersion onto the flake's surface.*

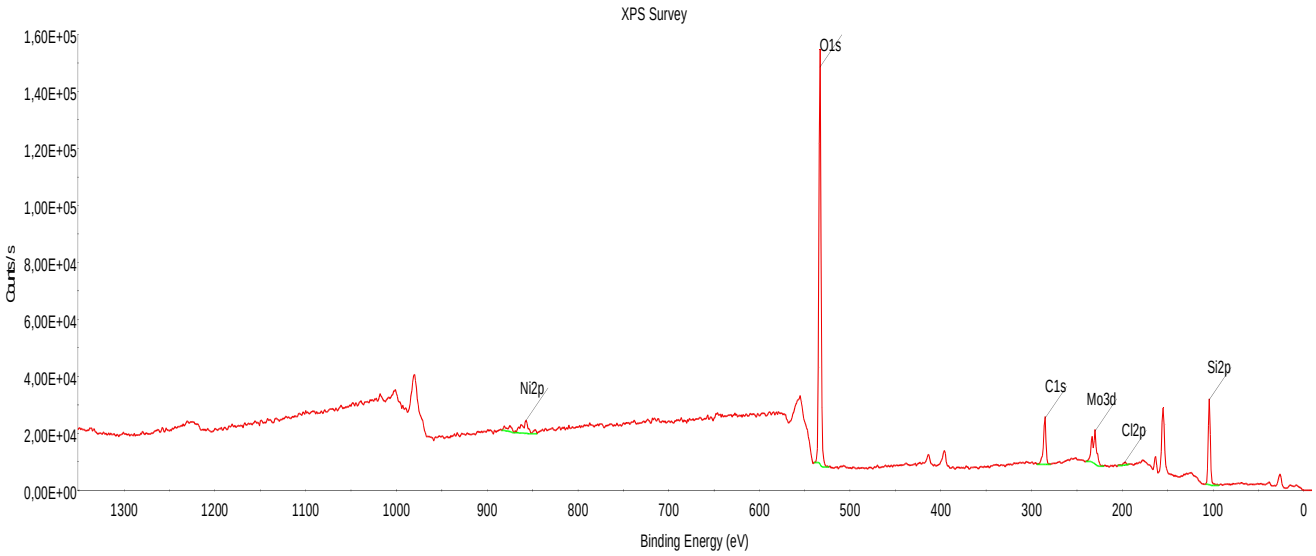

Figure S 7: *Survey XPS spectra of MoS_2-$NiCl_3$ samples showing the presence of MoS2 (Mo 3d and S 2p peaks), Ni (2p peak), and Cl (2p peak).*

Table S2: Atomic percentage calculated from the MoS_2-$NiCl_3$ XPS survey spectra.

Name	Peak BE	FWHM eV	Area (P) CPS.eV	Atomic %
O1s	533.11	2.81	407121.28	49.32
Si2p	104.03	2.82	83899.53	29.76
C1s	285.22	2.9	54949.48	17.17
Mo3d	230.12	3.33	65903.51	2.12
Ni2p	857.04	3.56	55668.4	1.13
Cl2p	197.49	3.71	3831.59	0.5

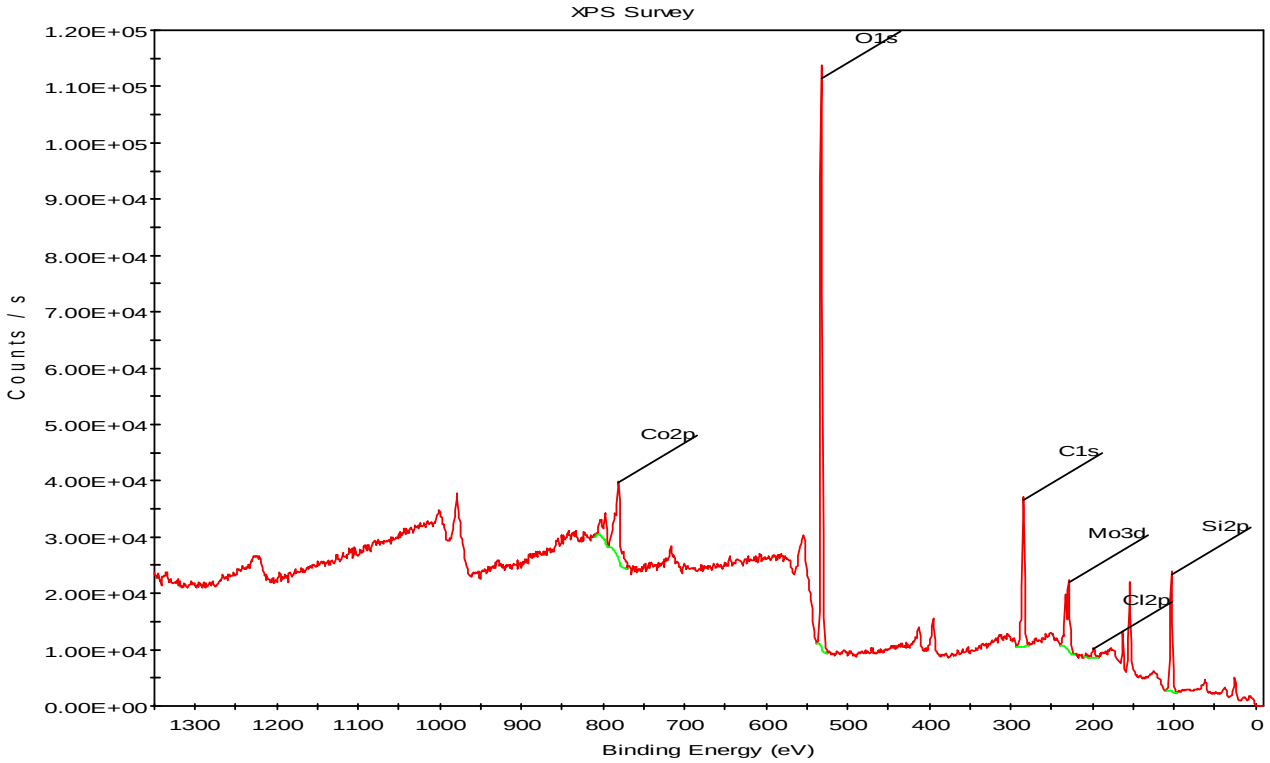

Figure S8: *Survey XPS spectra of MoS_2-$CoCl_3$ samples showing the presence of MoS2 (Mo 3d and S 2p peaks), Co (2p peak), and Cl (2p peak).*

Table S3: Atomic percentage calculated from the MoS_2-$CoCl_3$ XPS survey spectra.

Name	Peak BE	FWHM eV	Area (P) CPS.eV	Atomic %
O1s	532.1	3.002	315827.46	39.95
Si2p	103.09	2.937	63121.09	23.38
C1s	284.31	2.832	91342.13	29.79
Co2p	781.22	4.925	139550.87	3.21
Mo3d	229.21	3.207	72065.21	2.42
Cl2p	198.29	4.266	9115.36	1.25

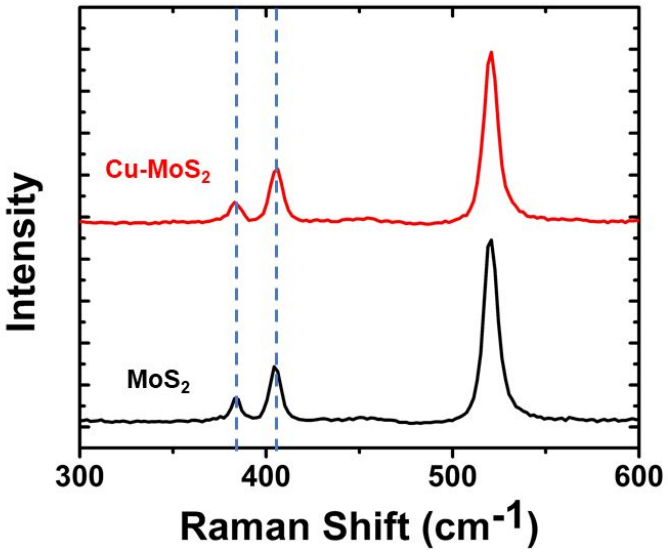

Figure S9: *Raman Spectra of pristine and Cu functionalized MoS_2. The MoS_2 signature peaks do not change in wavenumber or intensity after Cu functionalization, indicating the functionalization process do not alter the intrinsic structure of the MoS_2 lattice.*

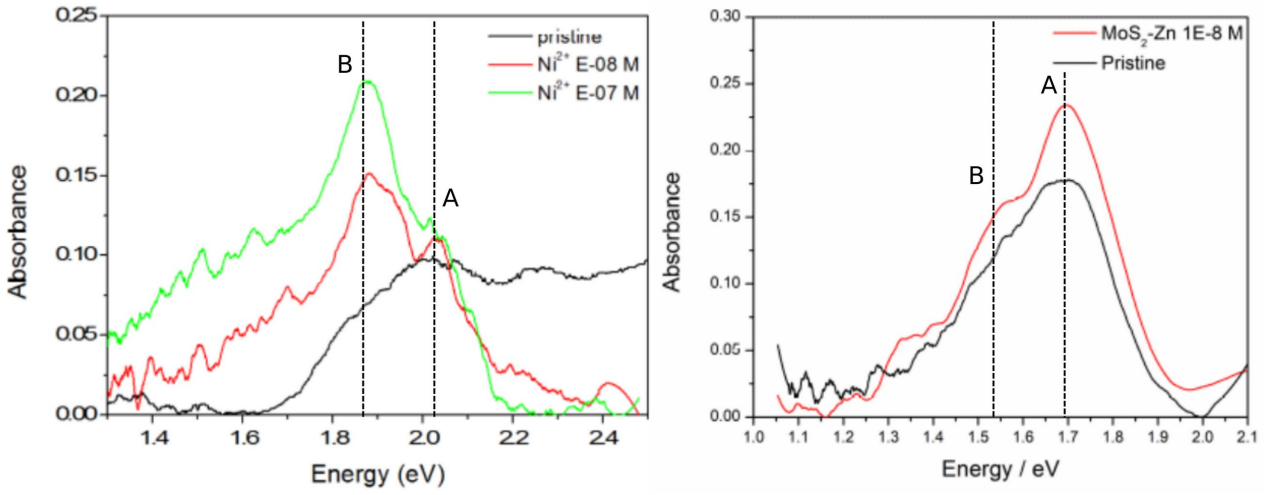

Figure S10: Room temperature absorbance spectra of the Ni-MoS_2 (right) and of Zn-MoS_2 (left) samples. A slight blue shift of the A and B excitons and new features associated with charge transfer transitions at energies lower than 1.6eV, are observed in the Ni-MoS2 samples, as expected from the electronic band structure for the complex in Figure 2 of the main text.

Reflectance spectra were collected with a 400-2400 nm supercontinuum laser source (NKT Photonics), focused through a Nikon TU Plan Fluor EPI 50x objective (NA 0.8). Signal was collected with a

Yokogawa Optical Spectrum Analyzer (OSA), with sensitivity ranging from 350-1200 nm. The reflected light was measured as-grown on SiO_2(300nm)/Si substrates, with an identical, clean substrate used for the calculation of reflectance through the relationship $Reflectance=I_{sample}/I_{substrate}$. Absorbance was calculated from reflectance using the relationship *Absorbance = -ln(10)*ln(Reflectance)*.

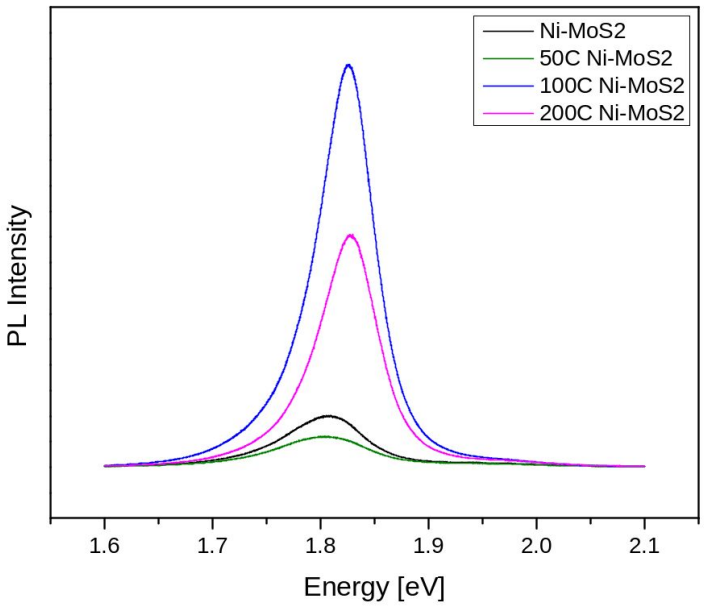

Figure S11: Photoluminescence spectrum of Ni functionalized MoS_2 monolayers at room temperature (black curve) and annealed at 50 ^oC (green curve), 100 ^oC (blue curve) and 200 ^oC (pink curve). Ni-MoS_2 samples at room temperature and annealed at 50 ^oC show exction/trion ratio close to 0.4 and FWHM of 320 meV. Ni-MoS_2 annealed at 100 and 200 ^oC show exction/trion ratio close to 1.6 and FWHM of 280 meV, similar to the pristine MoS_2.

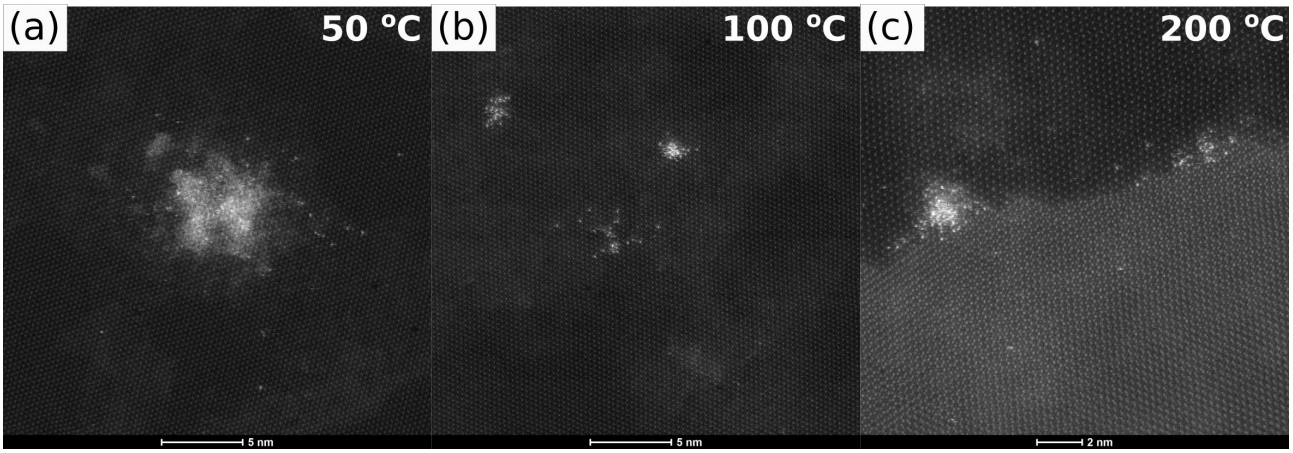

Figure S12: HAADF-STEM images of MoS_2 -Ni samples annealed at 50 ºC (a), 100 ºC (b) and 200 ºC (c), where the bright spots show Ni single atoms atomically dispersed on the MoS_2 basal plane and some clustering can be seen.